Inventory of Supplementary material:

I. Supplementary Figures S1-S9 and legends:

II. Supplementary Tables S1-S3:

III. Supplementary Methods (including Supplementary References)

IV. Supplementary Datasets S1 and S2:

Supplemental Dataset S1. Unbiased detection of H3K4m3, AcH3K9,14, AcH4K12 and AcH2B islands in hippocampal mouse chromatin (4 spreadsheets).

Supplemental Dataset S2. SICER comparison of acetylation profiles in hippocampal chromatin of TSA- and vehicle-treated animals (3 spreadsheets).

These datasets are accessible at the URL: http://in.umh.es/IP/Barco-lab-dataSets.html

Legends for Supplemental Figures S1-S9:

Supplemental Figure S1. Summary of the different gene expression and ChIP experiments presented in this study. Schema depicts a time line showing the times of TSA treatment, tissue collection and analytical procedures. Protein extracts from mouse hippocampus were used to assess histone modifications in bulk chromatin by western-blots at 15, 30, 75, 150 and 300 min after a single intraperitoneal TSA injection, and 30 and 150 min after vehicle administration. ChIPseq and ChIP assays were performed 30 min after TSA administration when histone hyperacetylation was at its peak. Whole-genome tiling arrays were used to profile gene expression 75 min after TSA or vehicle administration in wild-type and CBP heterozygous mice that were subjected or not to novelty exposure. TSA-triggered gene expression was measured by RT-qPCR at 75, 150 and 600 min after treatment, vehicle samples were taken 75 min after treatment.

Supplemental Figure S2. Testing of AcH2B antiserum. A. HEK293 cells were treated with TSA (2μM) or vehicle (Veh) for 2 h. Western blot analysis for AcH2B (AcH2B) was carried out in the presence of acetylated (Ac) or non-acetilated (Non Ac) peptide with the first 22 amino acids of mouse histone H2B. Peptide concentration was 2 μg/ml. β-actin was used as a loading control. **B.** HEK293 cells and mouse hippocampus protein extracts were immunoprecipitated with AcH2B antiserum (IP). Then, immunoprecipitated proteins were analysed by western blot using the same antiserum (AcH2B). Mock condition (Mock), rabbit IgG IPs (Control IgG) and whole lysate (Whole lysate) were loaded as controls. **C.** ChIP analysis was performed in mouse hippocampal chromatin extracts with anti-AcH2B (AcH2B) or preimmune serum (Prei). ChIP-PCRs were performed using primer pairs against the *Gapdh*, *Arc* and *Fos* gene promoters. The neuronal gene *Tubb5* and the gene *HBb-*

bh1, which is not expressed in mature neurons, were also analysed. PCR in the input condition (input) was performed using 1% of crude chromatin preparation.

Supplemental Figure S3. Reproducibility of ChIPseq experiments. A. Heatmap and hierarchical dendrogram depicting the cross-correlation matrix across the whole dataset for the entire set of samples. **B.** Two-dimensional Multi-Dimensional Scaling (MDS) of coverage profile across samples. **C.** A representative genomic view of ChIPseq data generated for H3K4me3, AcH3K9,14, AcH4K12, AcH2B and input are shown to illustrate reproducibility. **D.** Density heatmap showing the coverage across 10kb around Refseq TSSs. Individual sequences were binned in 50bp windows (200 bins per sequence) and coverage was computed and plotted as a relative color intensity scale.

Supplemental Figure S4. Correlation and overlap between epigenetic marks. A. Mean enrichment profiles presenting the genomic distribution of reads for AcH3K9,14, AcH4K12 and AcH2B across all annotated TSSs (left), the gene length (middle) or intergenic regions (right). The insets show a magnification of the scale in the Y-axis to better illustrate AcH4K12 and AcH2B profiles. **B.** Heatmap matrix of Pearson correlation indexes between the enrichment of different histone marks in the adult mouse hippocampus. The correlation was calculated for enrichment coverage values around the TSS (+/-1 kb) across all annotated TSS expressed as log2 enrichment over background level. **C.** Venn diagrams showing the overlap between the four types of islands. The values correspond to the number of islands that physically overlap (left) and to the number of genes containing islands (right).

Supplemental Figure S5. Correlation between epigenetic marks and gene expression levels. A. Heatmap showing signal density around all annotated TSSs (+/-10 kb) were subjected to k-means clustering for grouping those TSSs that presented

similar read densities for the different histone modifications (H3K4me3, AcH3K9,14, AcH4K12 and AcH2B). Linear normalization was applied to the datasets to reduce the bias caused by inter-samples intensity differences. The nine clusters initially identified were pooled into three groups according to their similarity after visual exploration. **B.** Boxplot shows relative mRNA expression values for genes in each of the clusters defined in A. **C.** A view of the acetylation profile in a fragment of chromosome 1 that contains genes with different levels of expression in hippocampal tissue illustrates the correlation between gene expression levels and the presence of the AcH3K9,14 mark. Island coloring follows Figure 2 legend.

Supplemental Figure S6. TSA hyperacetylation of bulk chromatin. Densitometric quantification of western blot data (**A**) and representative western blot images (**B**) of hippocampal bulk histone acetylation levels in animals subjected to intraperitoneal injection of TSA or vehicle (Veh) 30 minutes after injection. * $P < 0.05$, Student's t-test versus vehicle; n=3 per group. Data are expressed as mean ± s.e.m.

Supplemental Figure S7. TSA also targets intragenic sequences and putative regulatory regions. A. Mean enrichment pattern for AcH3K9,14 (red lines in upper panels), AcH4K12 (blue lines in middle panels) and AcH2B (green lines in bottom panels) were profiled across gene length (left) and intergenic regions (right) for vehicle- (dotted lines) and TSA-treated mice (solid lines). **B.** Mean enrichment pattern for AcH3K9,14 (red lines in upper panels), AcH4K12 (blue lines in middle panels) and AcH2B (green lines in bottom panels) were profiled across putative CBP (left) and p300 (right) enhancers in chromatin of vehicle- (dotted lines) and TSA-treated (solid lines) mice. Solid grey line in AcH3K9,14 and AcH4K12 ChIPseq experiments shows coverage in input condition. **C.** Mean enrichment pattern for AcH3K9,14 (red lines), AcH4K12 (blue lines) and AcH2B (green lines) in intergenic islands that are

not associated with annotated genes nor CBP/p300 putative enhancers in the chromatin of vehicle- (dotted lines) and TSA-treated (solid lines) mice. Solid grey shows the coverage in input condition. These 2987 islands were initially identified based on significant AcH3K9,14 enrichment but they were also enriched in AcH4K12 and AcH2B. **D.** Representative genomic view presenting some intergenic acetylation islands. These islands may label non annotated genes or indicate the existence of novel regulatory regions.

Supplemental Figure S8. Correlation between the changes in histone acetylation and transcript levels induced by TSA. A. Pie chart showing annotation of top differentially enriched islands upon TSA administration relative to their location within the gene sequence. Most of the largest changes in AcH3 and AcH4 occurred at promoter regions (5' UTR), whereas, the largest changes in AcH2B levels occurred at internal positions (Intragenic). Very few of these large changes mapped into the 3' UTR (3' UTR). **B.** Scatter plots show differential expression values in genes that were on the top of differentially acetylated genes upon TSA treatment. Linear regression model is shown as a red line. Pearson correlation coefficients are also included (top of each chart). **C.** Scatter plots show differential acetylation values in the genes that were differentially expressed genes upon TSA treatment. Red points correspond to genes that were also present in the group of genes that showed the largest acetylation response upon TSA administration (FC> 2, FDR p-val.< 10^{-10} in the comparison of TSA and vehicle samples). Most red points in the AcH3 and AcH4 graphs correspond to the same genes; among them we find *Rest*, *L3mbtl3*, *Sox11*, *Fam60*. Linear regression model is shown as a red line. Pearson correlation coefficients are also included (top of each chart).

Supplemental Figure S9. Interaction between TSA-induced hyperacetylation and novelty-driven gene expression. A. Box plot depicts enrichment levels for each histone mark in NE-induced genes. Enrichment levels for the population of islands found for each modification is also included as reference (All peaks). Percentages represent the number of genes showing enriched islands among NE-induced genes. **B.** Scatter plots show differential acetylation values as fold changes (log2) and gene expression fold changes (mRNA, log2) in the comparison of TSA and vehicle, in genes that were differentially expressed genes upon novelty. Linear regression model is shown as a red line. Pearson correlation coefficients are also included (top of each chart).

Lopez-Atalaya et al., Suplemental Figure S1

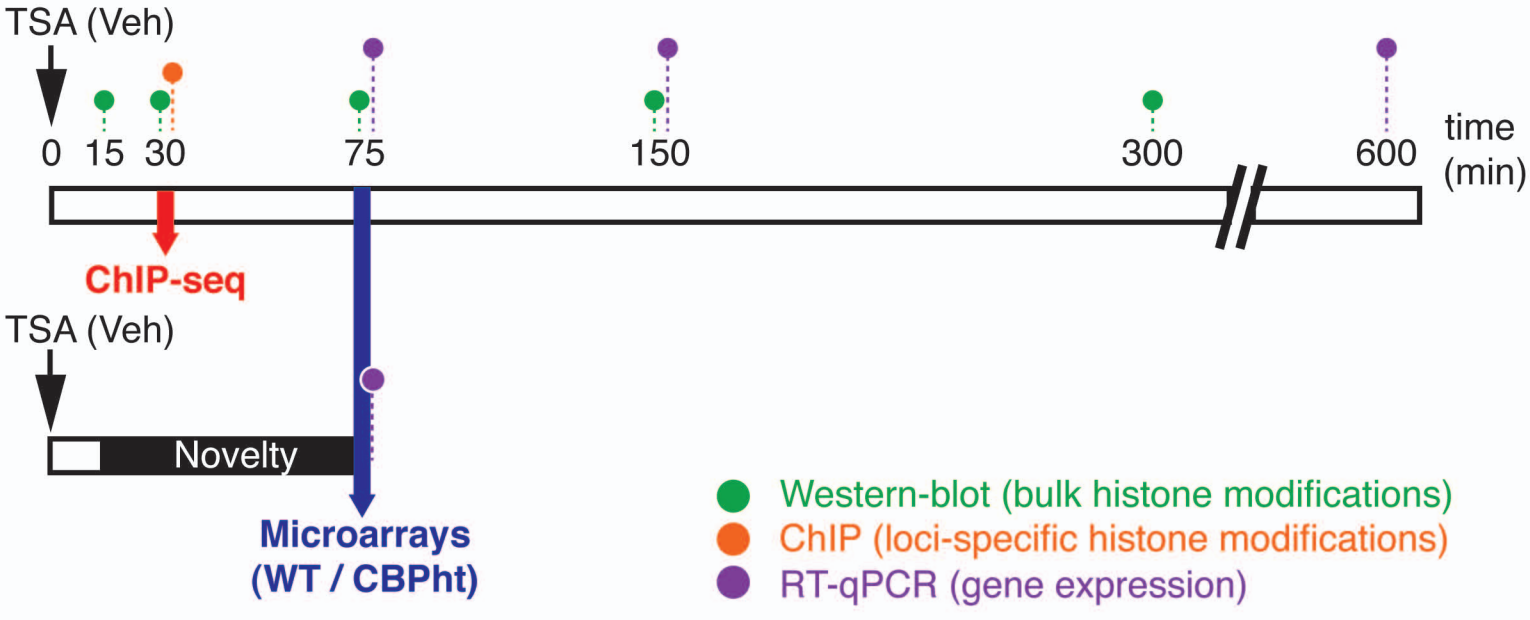

Lopez-Atalaya et al., Supplemental Figure S2

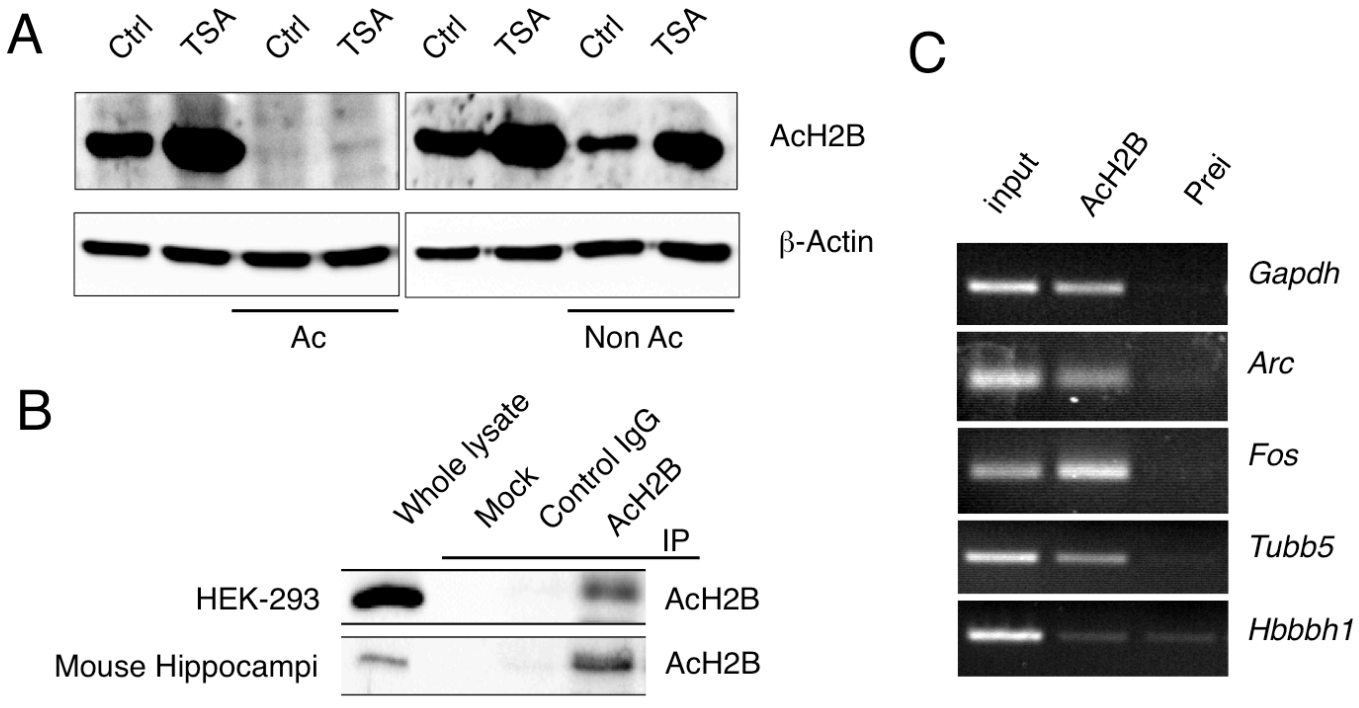

Lopez-Atalaya et al., Supplemental Figure S3

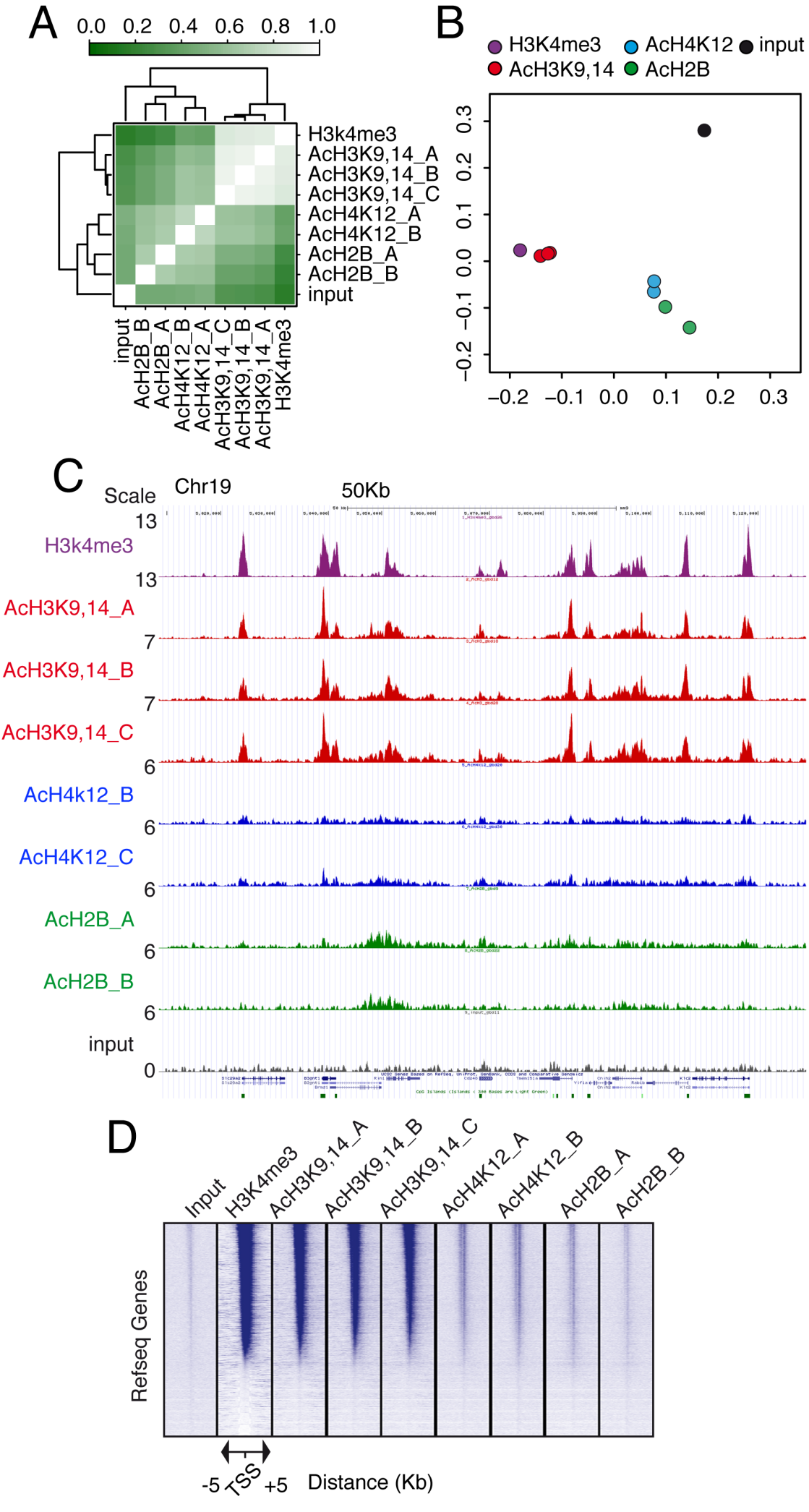

Lopez-Atalaya et al., Supplemental Figure S4

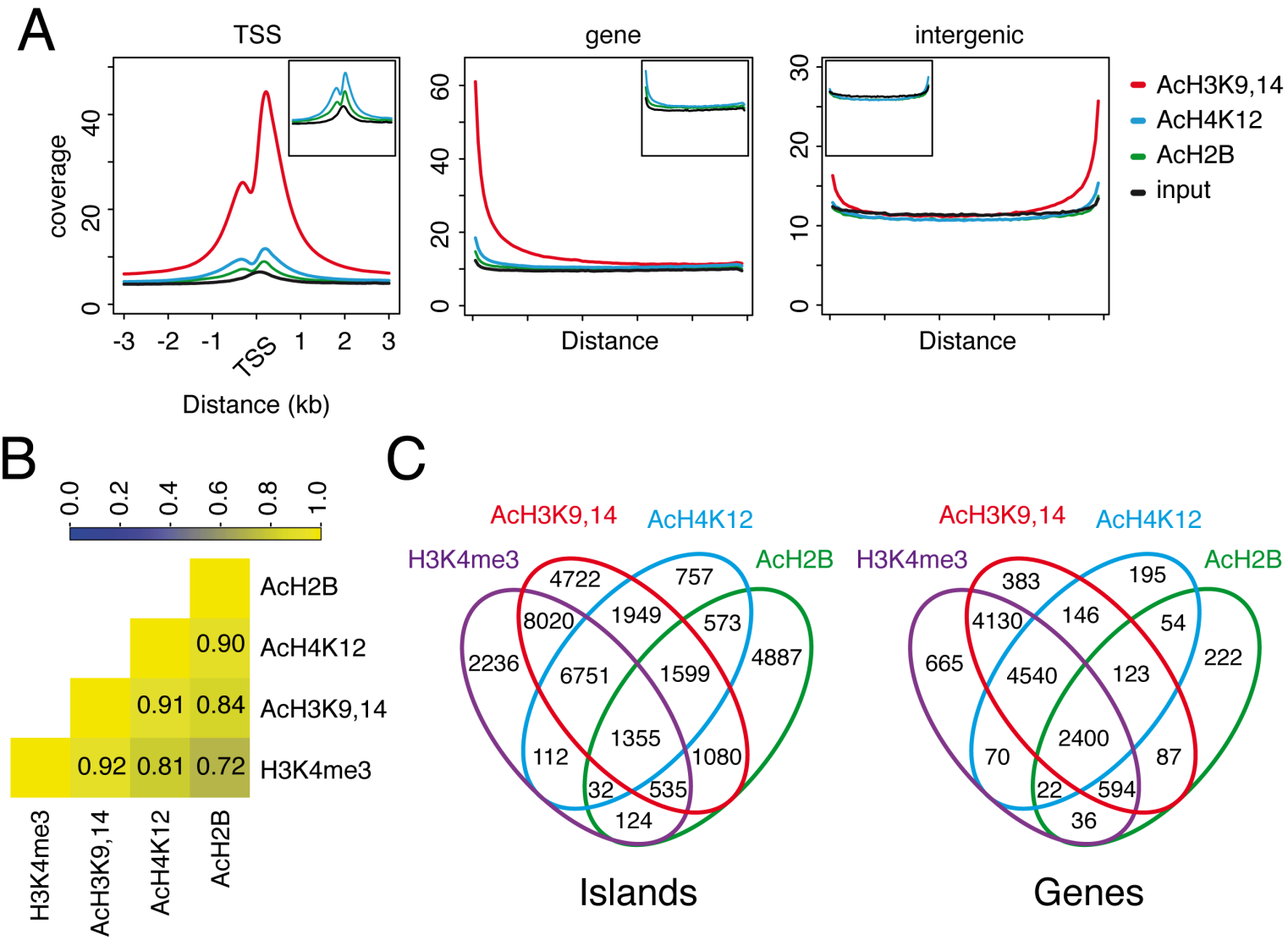

Lopez-Atalaya et al., Supplemental Figure S5

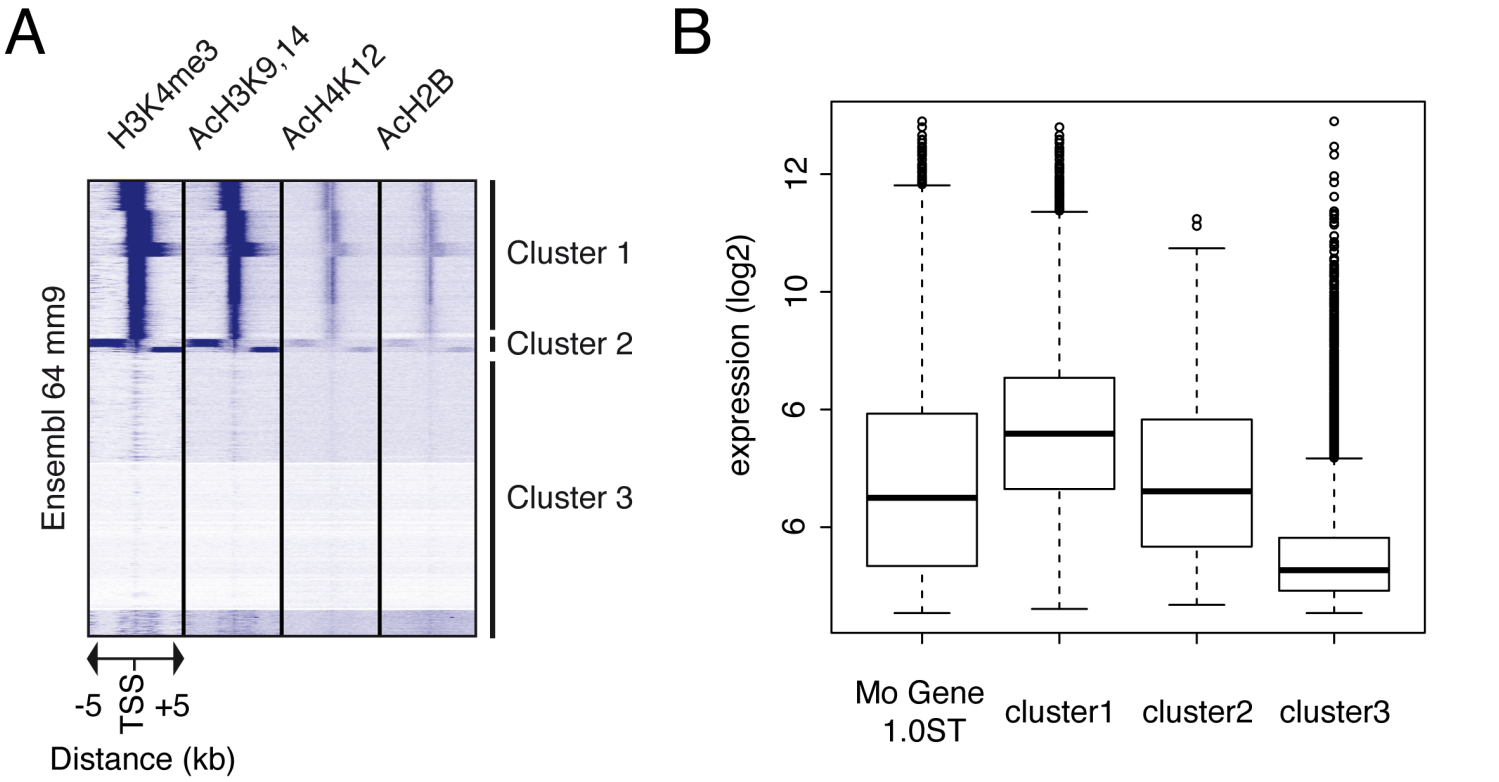

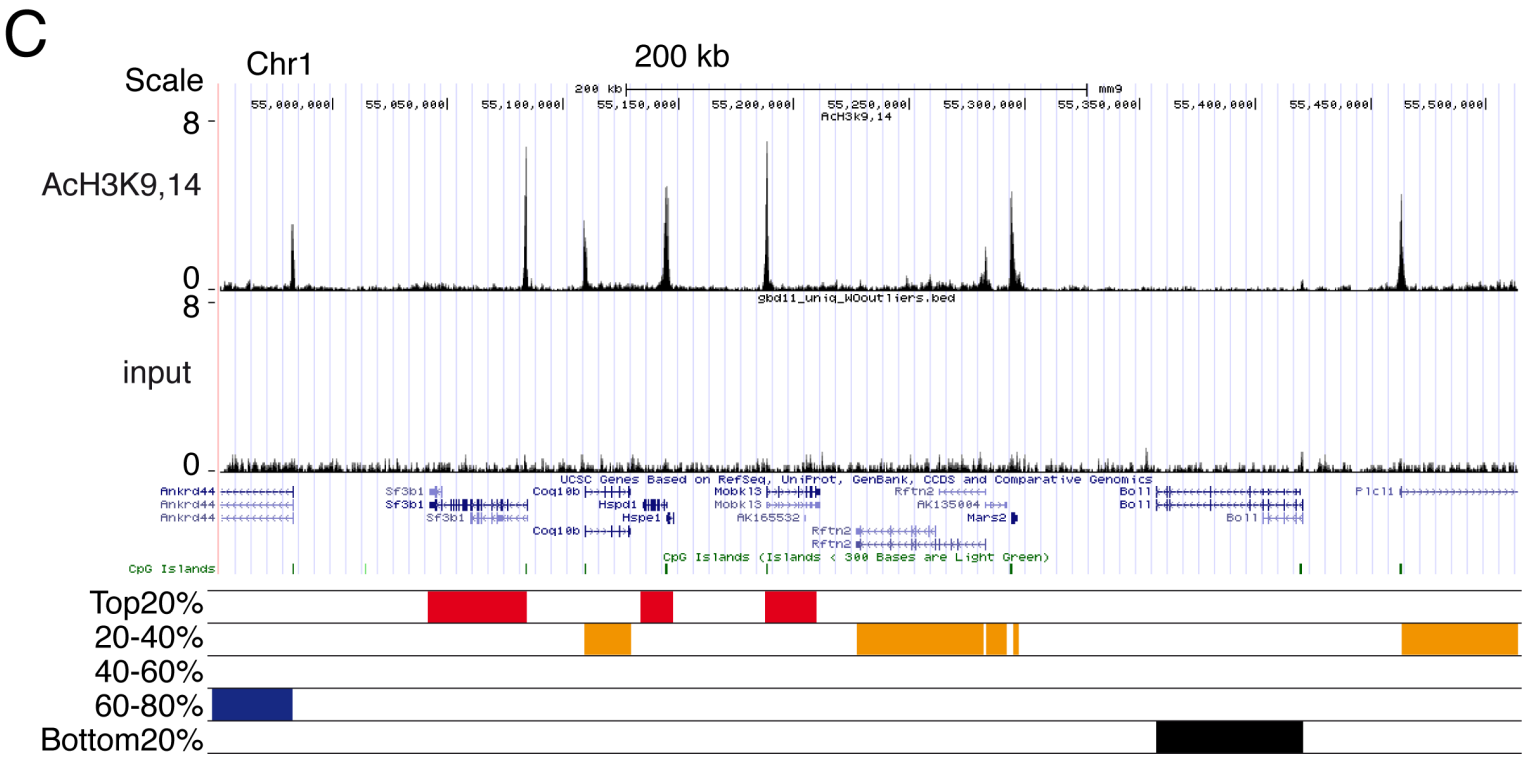

Lopez-Atalaya et al., Supplemental Figure S6

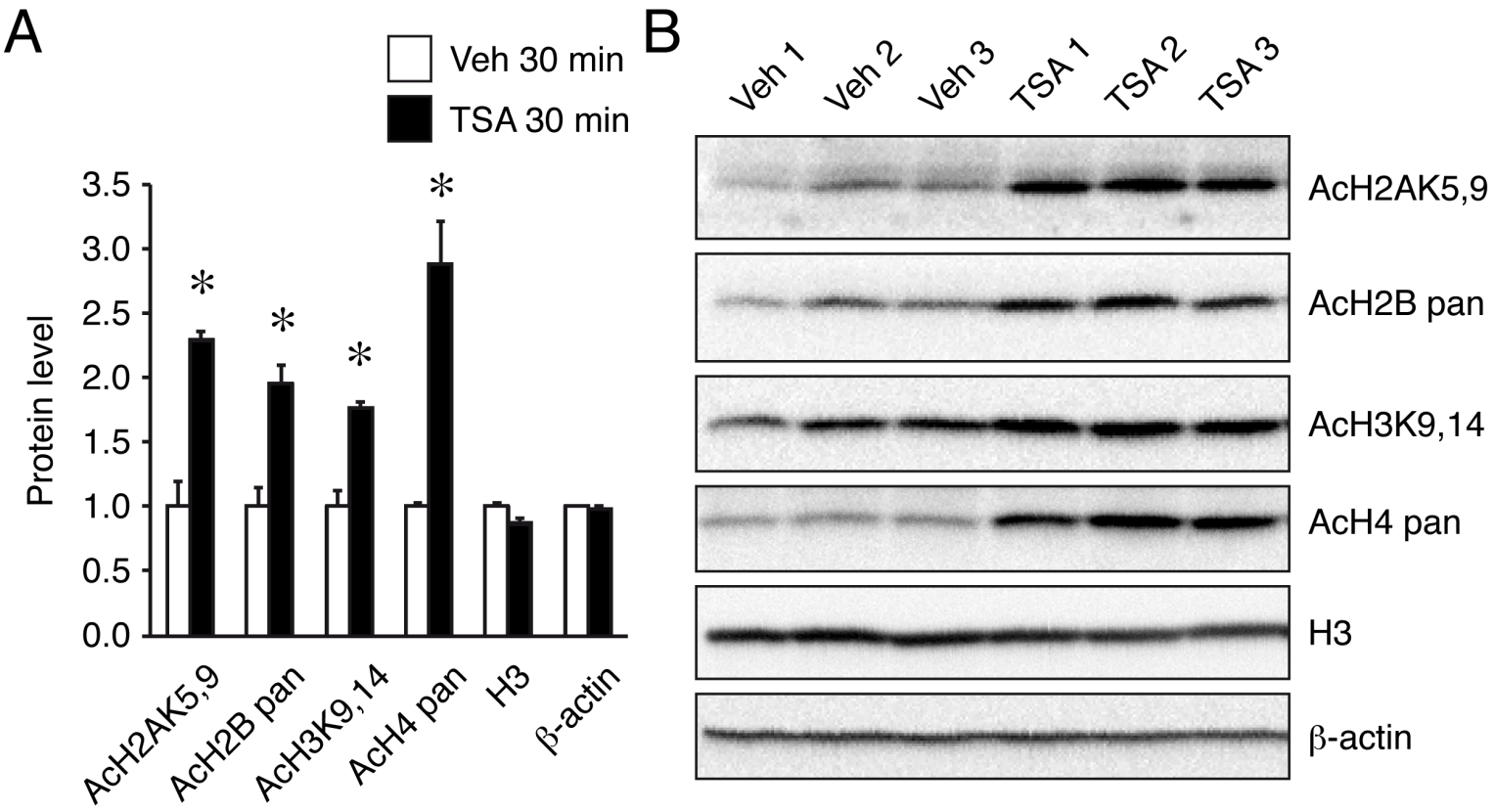

Lopez-Atalaya et al., Supplemental Figure S7

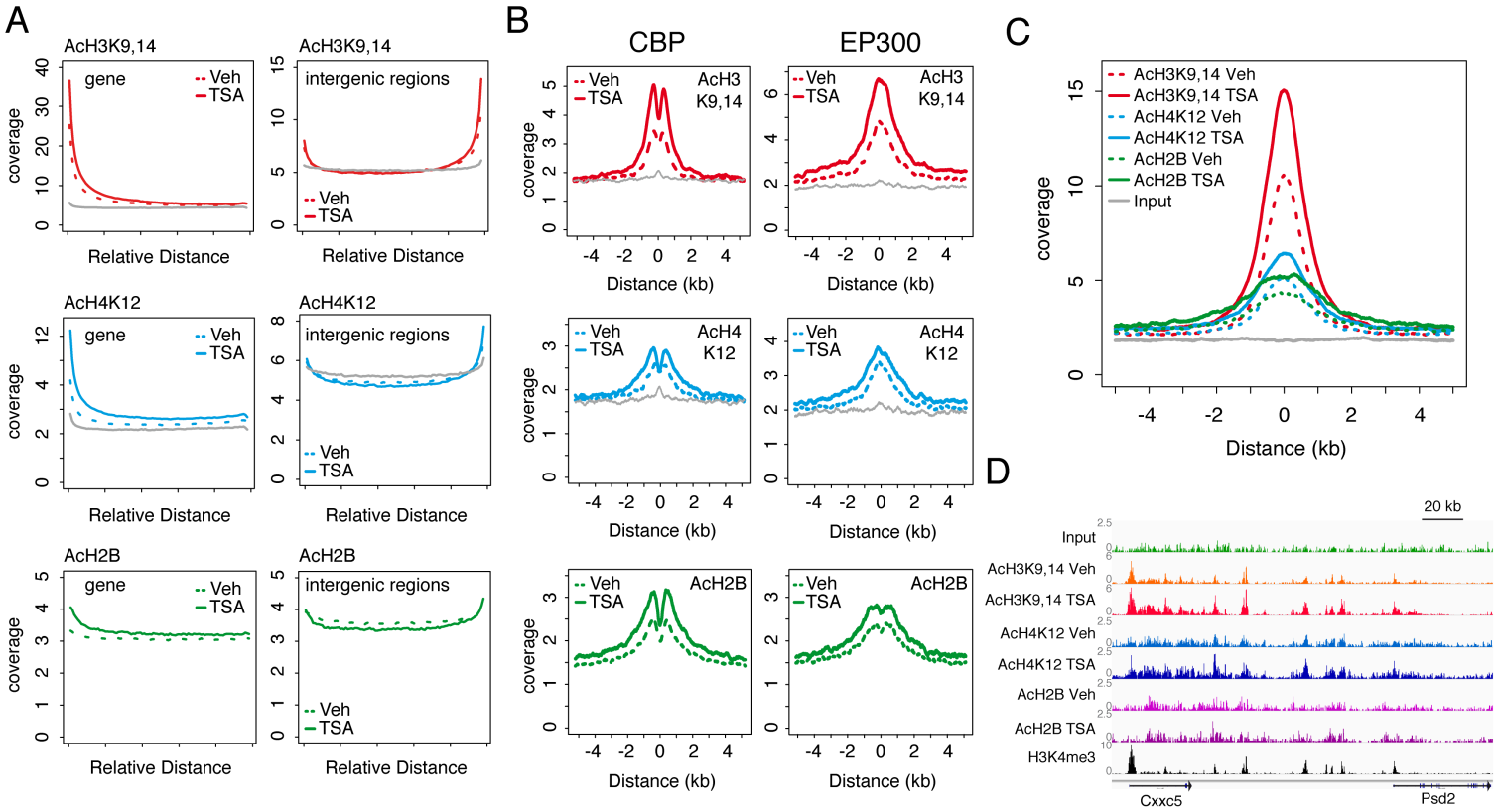

Lopez-Atalaya et al., Supplemental Figure S8

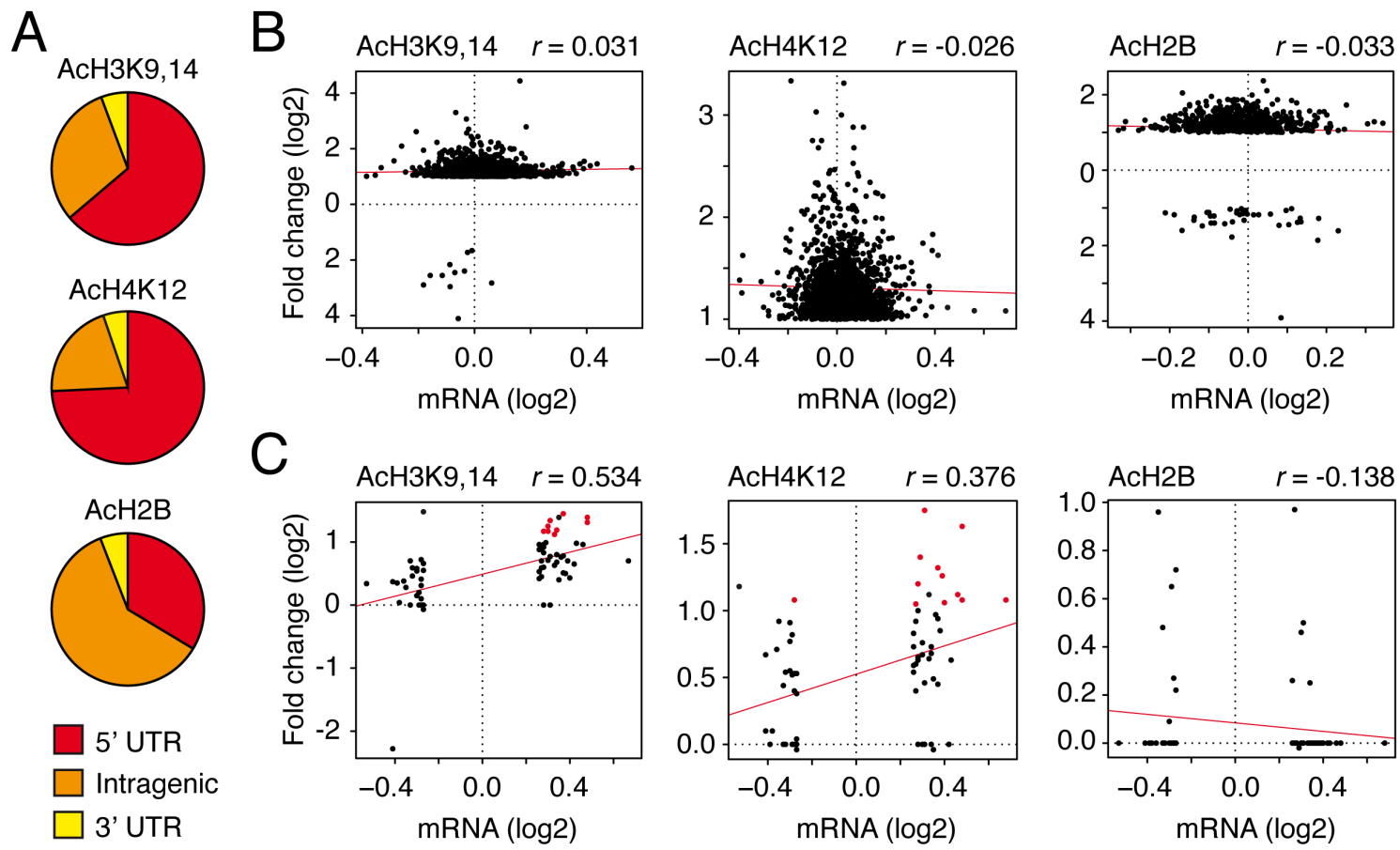

Lopez-Atalaya et al., Supplemental Figure S9

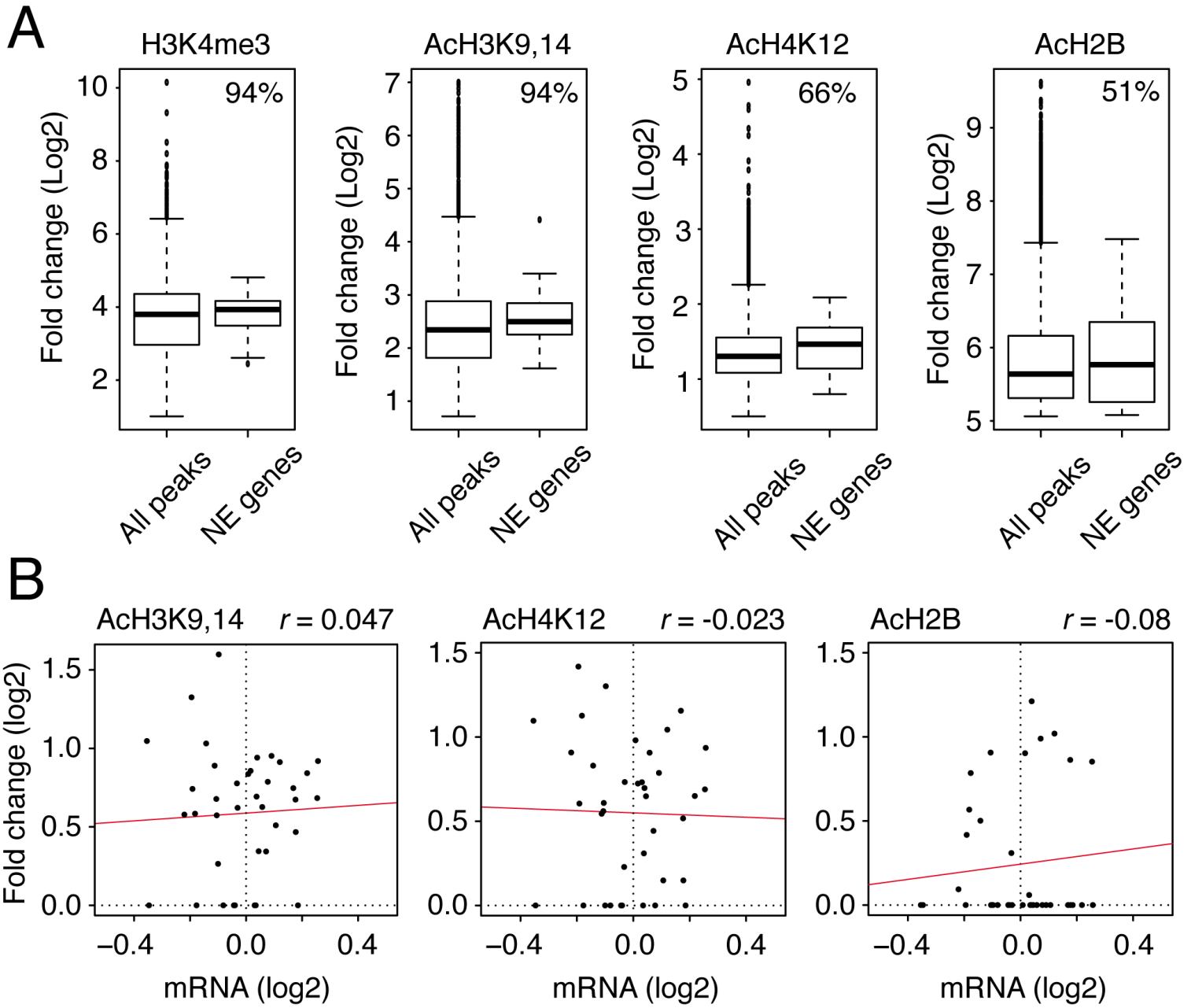

Supplemental Table S1. ChIPseq library size, technology and other features.

Label	Ab	Name	#map	%unique	Nº READS	READ length	Sequencing kit	Instrument
GBD-1	AcH2B_pan	Vehicle_1	5181299	84.0%	4353626	36	Scanning buffer v2.0	GAII
GBD-3	AcH2B_pan	Vehicle_2	7738581	85.4%	6612593	36	Chrysalis 36cycles v2.0	GAII
GBD-5	AcH2B_pan	TSA	7308482	87.0%	6356199	36	Chrysalis 36cycles v2.2	GAII
GBD-9	AcH2B_pan	naïve_A	9770926	88.1%	8611330	50	TruSeq™ SBS v5	Hi-seq 2000
GBD-22	AcH2B_pan	naïve_B	8658059	86.4%	7483585	50	TruSeq™ SBS v5	Hi-seq 2000
GBD-12	AcH3_K9,14	naïve_A	8237201	90.3%	7439053	50	TruSeq™ SBS v5	Hi-seq 2000
GBD-28	AcH3_K9,14	naïve_C	13867710	88.3%	12240918	50	TruSeq™ SBS v3	Hi-seq 2000
GBD-18	AcH3_K9,14	Vehicle	18156557	88.8%	16125373	50	TruSeq™ SBS v3	Hi-seq 2000
GBD-19	AcH3_K9,14	TSA	17985333	90.7%	16306398	50	TruSeq™ SBS v3	Hi-seq 2000
GBD-30	AcH4_K12	naïve_A	14187515	85.6%	12142545	50	TruSeq™ SBS v3	Hi-seq 2000
GBD-20	AcH4_K12	Vehicle	18009133	85.6%	15422864	50	TruSeq™ SBS v3	Hi-seq 2000
GBD-21	AcH4_K12	TSA	18283124	87.4%	15984775	50	TruSeq™ SBS v3	Hi-seq 2000
GBD-26	H3K4me3	naïve	9536718	87.4%	8338374	50	TruSeq™ SBS v3	Hi-seq 2000
GBD-11	None	Input_veh	7904594	79.7%	6297496	50	TruSeq™ SBS v5	Hi-seq 2000
GBD-24	IgG	naïve	9220090	79.6%	7339222	50	TruSeq™ SBS v3	Hi-seq 2000

ChIP grade IgG	Type	Form	Host	Reference
H3-K4me3	Polyclonal	affinity purified	Rabbit	**http://www.millipore.com/catalogue/item/07-473#**
Ac-H3 -K9,14	Polyclonal	purified	Rabbit	**http://www.millipore.com/catalogue/item/06-599**
Ac-H4-K12	Polyclonal	whole antiserum	Rabbit	**http://www.abcam.com/Histone-H4-acetyl-K12-antibody-ab46983.html**
AcH2B-pan	Polyclonal	whole antiserum	Rabbit	Barco Lab (Immunogen: S**k**SAPAPK**k**GS**k**KAIT**k**AQGSC-KLH) k=AcK pos. 5,12,15 and 20

Supplemental Table S2. Comparison of gene expression profiles in the hippocampus of TSA- and vehicle-treated animals.

Table shows the differential expression analysis of vehicle versus TSA (2.4mg/kg i.p; 30 min) samples using GeneSpring software (FDR< 0,05 FC>1.2).

Transcripts Cluster Id	total_probes	genesymbol	Fold change	Corrected p-value	p-value	genedescription
10510254	25	Fv1	1.61	0.0318	4.70E-04	Friend virus susceptibility 1
10396270	34	Dact1	1.40	0.0019	2.48E-06	dapper homolog 1, antagonist of beta-catenin (xenopus)
10522712	25	Rest	1.40	0.0162	1.14E-04	RE1-silencing transcription factor
10399725	27	Sox11	1.38	0.0363	5.76E-04	SRY-box containing gene 11
10432236	30	Rnd1	1.34	0.0189	1.47E-04	Rho family GTPase 1
10493245	25	Mex3a	1.34	0.0363	5.77E-04	mex3 homolog A (C. elegans)
10592719	25	Oaf	1.32	0.0423	7.60E-04	OAF homolog (Drosophila)
10448506	40	Ccnf	1.31	0.0211	1.92E-04	cyclin F
10554693	28	Stard5	1.30	0.0252	2.68E-04	StAR-related lipid transfer (START) domain containing 5
10368380	48	L3mbtl3	1.29	0.0171	1.28E-04	l(3)mbt-like 3 (Drosophila)
10534041	31	Stx2	1.29	0.0033	5.92E-06	syntaxin 2
10505270	26	Slc31a2	1.29	0.0459	9.42E-04	solute carrier family 31, member 2
10400971	27	Six4	1.28	0.0039	8.45E-06	sine oculis-related homeobox 4 homolog (Drosophila)
10464659	35	Rad9	1.28	0.0129	7.15E-05	RAD9 homolog (S. pombe)
10500011	17	Tuft1	1.27	0.0469	9.86E-04	tuftelin 1
10387638	35	Fgf11	1.27	0.0245	2.52E-04	fibroblast growth factor 11
10550597	26	Fbxo46	1.26	0.0498	1.11E-03	F-box protein 46
10485170	34	Cry2	1.26	0.0269	3.33E-04	cryptochrome 2 (photolyase-like)
10568228	20	Zfp747	1.26	0.0268	3.27E-04	zinc finger protein 747
10398751	28	Zfyve21	1.25	0.0074	2.70E-05	zinc finger, FYVE domain containing 21
10549497	39	Fam60a	1.24	0.0245	2.56E-04	family with sequence similarity 60, member A
10442454	27	Pgp	1.24	0.0431	8.04E-04	phosphoglycolate phosphatase
10436442	37	Fam60a	1.24	0.0018	1.88E-06	family with sequence similarity 60, member A
10472923	26	Ak3l1	1.24	0.0019	2.65E-06	adenylate kinase 3-like 1
10382470	30	Tmem104	1.24	0.0270	3.39E-04	transmembrane protein 104
10599514	30	Bcorl1	1.23	0.0427	7.82E-04	BCL6 co-repressor-like 1
10435641	36	Fstl1	1.23	0.0317	4.66E-04	follistatin-like 1
10373515	25	Suox	1.23	0.0474	1.01E-03	sulfite oxidase
10489958	25	Kcng1	1.23	0.0457	9.24E-04	potassium voltage-gated channel, subfamily G, member 1
10416736	31	6720463M24Rik	1.22	0.0370	6.04E-04	RIKEN cDNA 6720463M24 gene
10589958	14	Gm9487	1.22	0.0237	2.37E-04	glyceraldehyde-3-phosphate dehydrogenase pseudogene
10551496	27	Paf1	1.22	0.0463	9.64E-04	
10529028	19	2310016E02RiklAgbl5	1.21	0.0033	5.70E-06	RIKEN cDNA 2310016E02 gene l ATP/GTP binding protein-like 5
10379436	32	Rhbdl3	1.21	0.0080	3.12E-05	rhomboid, veinlet-like 3 (Drosophila)

10545130	25	Gadd45a	1.21	0.0498	1.12E-03	growth arrest and DNA-damage-inducible 45 alpha
10445688	23	Ccnd3	1.21	0.0457	9.30E-04	cyclin D3
10497237	30	Pag1	1.21	0.0252	2.78E-04	phosphoprotein associated with glycosphingolipid microdomains 1
10471525	31	Ptrh1|Stxbp1|1700019L03Rik	1.21	0.0423	7.68E-04	peptidyl-tRNA hydrolase 1 homolog (S. cerevisiae) | syntaxin binding protein 1 | RIKEN cDNA 1700019L03 gene
10463515	25	Hps6	1.21	0.0132	7.42E-05	Hermansky-Pudlak syndrome 6
10493309	29	Rit1	1.20	0.0040	8.98E-06	Ras-like without CAAX 1
10547641	38	Slc2a3	1.20	0.0429	7.95E-04	solute carrier family 2 (facilitated glucose transporter), member 3
10572419	36	Ell	1.20	0.0181	1.38E-04	elongation factor RNA polymerase II
10366983	38	Tmem194	1.20	0.0362	5.68E-04	transmembrane protein 194
10489368	25	Fitm2|2310001K24Rik	1.20	0.0016	1.42E-06	fat storage-inducing transmembrane protein 2 | RIKEN cDNA 2310001K24 gene
10526838	25	Got2	-1.20	0.0202	1.69E-04	glutamate oxaloacetate transaminase 2, mitochondrial
10585974	25	Myo9a	-1.20	0.0041	9.70E-06	myosin IXa
10516211	11	Ndufs5	-1.21	0.0016	1.32E-06	NADH dehydrogenase (ubiquinone) Fe-S protein 5
10466886	25		-1.21	0.0211	1.89E-04	
10526311	29	Bcl7b	-1.21	0.0210	1.81E-04	B-cell CLL/lymphoma 7B
10584071	46	Prdm10	-1.21	0.0084	3.52E-05	PR domain containing 10
10589982	30	Azi2	-1.21	0.0162	1.13E-04	5-azacytidine induced gene 2
10382104	25	Snord104	-1.21	0.0135	8.01E-05	small nucleolar RNA, C/D box 104
10397083	27	Rbm25	-1.21	0.0263	3.06E-04	RNA binding motif protein 25
10584350	26	Tpt1|Tpt1pl|Gm6790	-1.21	0.0344	5.24E-04	tumor protein, translationally-controlled 1 | tumor protein, translationally-controlled 1 pseudogene
10563955	24	Gm3079	-1.21	0.0449	8.54E-04	predicted gene 3079
10469035	30	Sephs1	-1.21	0.0427	7.88E-04	selenophosphate synthetase 1
10450752	32	Trim39	-1.21	0.0139	8.65E-05	tripartite motif-containing 39
10395628	30	Scfd1	-1.22	0.0074	2.69E-05	Sec1 family domain containing 1
10402473	32	Clmn	-1.22	0.0017	1.55E-06	calmin
10404053	13	Hist1h2bc	-1.22	0.0252	2.78E-04	histone cluster 1, H2bc
10416496	42	Tpt1|Tpt1p	-1.22	0.0224	2.12E-04	tumor protein, translationally-controlled 1 | tumor protein, translationally-controlled 1 pseudogene
10563965	29		-1.22	0.0252	2.72E-04	
10564043	29		-1.22	0.0263	3.10E-04	
10563967	29		-1.22	0.0259	2.94E-04	
10563971	29		-1.22	0.0259	2.96E-04	
10564013	27	Snord115	-1.22	0.0211	1.88E-04	Small nucleolar RNA, C/D Box 115 cluster
10564017	27	Snord115	-1.22	0.0218	2.06E-04	Small nucleolar RNA, C/D Box 115 cluster
10345620	19	Mrpl30	-1.22	0.0344	5.20E-04	mitochondrial ribosomal protein L30
10564033	26		-1.23	0.0465	9.76E-04	
10564023	24		-1.23	0.0370	6.02E-04	
10454525	33	Iws1	-1.23	0.0350	5.40E-04	IWS1 homolog (S. cerevisiae)
10423647	31	Kcns2	-1.23	0.0218	2.05E-04	K+ voltage-gated channel, subfamily S, 2

10429491	26	Arc	-1.23	0.0048	1.34E-05	activity regulated cytoskeletal-associated protein
10545515	29	Dnahc6	-1.25	0.0036	7.13E-06	dynein, axonemal, heavy chain 6
10563907	26		-1.25	0.0411	7.24E-04	
10563905	26		-1.25	0.0411	7.27E-04	
10516867	35	Gmeb1	-1.25	0.0268	3.31E-04	glucocorticoid modulatory element binding protein 1
10557655	47	Srcap	-1.26	0.0265	3.16E-04	Snf2-related CREBBP activator protein
10402080	30	BC002230	-1.26	0.0462	9.58E-04	
10545502	30	Dnahc6	-1.27	0.0457	9.07E-04	dynein, axonemal, heavy chain 6
10457302	39	Epc1	-1.27	0.0080	3.19E-05	enhancer of polycomb homolog 1 (Drosophila)
10490653	27	Gmeb2	-1.28	0.0039	7.98E-06	glucocorticoid modulatory element binding protein 2
10444957	38	Ppp1r10	-1.30	0.0048	1.38E-05	protein phosphatase 1, regulatory subunit 10
10346914	25	Fastkd2	-1.31	0.0132	7.44E-05	FAST kinase domains 2
10459602	25	Ptpn2	-1.33	0.0190	1.49E-04	protein tyrosine phosphatase, non-receptor type 2
10520388	25	Rbm33	-1.33	0.0319	4.72E-04	RNA binding motif protein 33
10598089	25		-1.39	0.0414	7.36E-04	
10460202	36	Suv420h1	-1.44	0.0356	5.54E-04	suppressor of variegation 4-20 homolog 1 (Drosophila)

Supplemental Table S3. Comparison of gene expression profiles in the hippocampus of wild-type and cbp+/- mice that were treated with TSA- or vehicle and subjected or not to novelty exposure.

Three-way ANOVA analysis of differential expression in wild-type and cbp+/- mice treated with vehicle (VEH) or TSA (2.4mg/kg i.p; 30 min) that were subjected to 1 h novelty exposure (NE) or kept in their home cage (HC). GeneSpring software, FDR< 0,05 FC>1.2. Condition variables: cbp+/- (CBP) or wild-type (WT); home cage (HC) or novelty exposure (NE); Treatment variables: vehicle (VEH) or TSA.

TCID	genesymbol	FC_CBP-TSA-NE	FC_CBP-TSA-SC	FC_CBP-VEH-NE	FC_CBP-VEH-SC	FC_WT-TSA-NE	FC_WT-TSA-SC	FC_WT-VEH-NE	FC_WT-VEH-SC	FDR (Condition)	FDR (Condition-Genotype)	FDR (Condition-Genotype-Treatment)	FDR (Condition-Treatment)	FDR (Genotype)	FDR (Genotype-Treatment)	FDR (Treatment)
10464905	Npas4	2.22	0.83	2.33	0.97	2.87	0.87	2.94	1.00	1.07E-12	NS	1.00	1.00	0.24	0.99	0.36
10429491	Arc	1.81	0.87	2.14	1.02	2.06	0.85	2.27	1.00	9.42E-10	1.00	1.00	1.00	0.97	0.98	0.12
10363735	Egr2	2.00	1.05	2.39	0.96	2.13	0.95	2.19	1.00	1.19E-08	1.00	1.00	1.00	1.00	0.99	0.93
10401841	Dio2	1.47	0.94	1.39	0.89	1.61	0.96	1.63	1.00	6.42E-08	1.00	1.00	1.00	0.43	0.98	0.99
10427035	Nr4a1	1.84	0.90	1.94	1.01	2.20	0.94	2.09	1.00	1.05E-07	1.00	1.00	1.00	0.88	0.98	0.93
10504838	Nr4a3	1.45	1.12	1.52	1.00	1.36	0.98	1.33	1.00	1.05E-07	1.00	1.00	1.00	0.27	0.98	0.95
10560481	Fosb	1.83	0.99	2.02	0.93	2.15	1.07	2.03	1.00	1.05E-07	1.00	1.00	1.00	0.83	0.98	0.99
10504218	Dnajb5	1.25	1.06	1.39	1.09	1.26	1.02	1.33	1.00	1.29E-06	1.00	1.00	1.00	0.68	0.98	0.41
10482772	Nr4a2	1.29	0.97	1.37	0.95	1.46	1.06	1.42	1.00	2.02E-06	1.00	1.00	1.00	0.54	0.98	0.99
10397346	Fos	1.73	0.82	2.02	1.01	1.94	0.90	2.18	1.00	2.15E-06	1.00	1.00	1.00	0.96	0.98	0.41
10454782	Egr1	1.67	0.92	1.67	1.03	1.73	1.04	1.81	1.00	7.00E-06	1.00	1.00	1.00	0.96	0.99	0.98
10406626	Homer1	1.41	1.05	1.49	0.99	1.30	0.92	1.33	1.00	1.36E-05	1.00	1.00	1.00	0.64	0.98	0.96
10471586	Hspa5	1.37	1.20	1.41	1.08	1.47	1.06	1.43	1.00	1.46E-05	1.00	1.00	1.00	0.95	1.00	0.75
10458555	Spry4	1.23	1.02	1.17	1.02	1.26	0.96	1.17	1.00	7.20E-05	1.00	1.00	1.00	1.00	0.99	0.93
10449284	Dusp1	1.24	0.70	1.35	0.92	1.79	0.88	2.18	1.00	1.17E-04	1.00	1.00	1.00	0.18	0.99	0.36
10545859	Egr4	1.47	0.95	1.50	0.99	1.64	1.14	1.54	1.00	1.30E-04	1.00	1.00	1.00	0.79	0.98	0.96
10527332	Nptx2	1.19	1.04	1.32	1.02	1.43	0.98	1.31	1.00	1.54E-04	1.00	1.00	1.00	1.00	0.98	1.00
10584578	Hspa8	1.42	1.01	1.56	1.06	1.26	0.81	1.66	1.00	1.68E-04	1.00	1.00	1.00	0.79	0.98	0.16
10395136		1.37	1.09	1.37	1.05	1.36	1.08	1.48	1.00	1.78E-04	1.00	1.00	1.00	1.00	0.99	0.99
10584576	Hspa8	1.41	1.01	1.55	1.06	1.26	0.80	1.65	1.00	2.07E-04	1.00	1.00	1.00	0.82	0.98	0.17
10584580		1.37	0.83	1.68	1.04	1.35	0.79	1.63	1.00	2.74E-04	1.00	1.00	1.00	1.00	1.00	0.12
10467206	Ppp1r3c	1.11	0.88	1.12	0.86	1.10	0.97	1.32	1.00	3.05E-04	1.00	1.00	1.00	0.31	0.98	0.62
10401743	1933437F05Rik	1.37	1.10	1.43	1.06	1.39	1.00	1.42	1.00	4.35E-04	1.00	1.00	1.00	0.96	0.99	1.00
10403743	Inhba	1.30	0.92	1.43	0.93	1.48	1.02	1.48	1.00	4.36E-04	1.00	1.00	1.00	0.81	0.98	0.99
10357875	Btg2	1.22	0.89	1.36	0.91	1.37	0.94	1.29	1.00	4.59E-04	1.00	1.00	1.00	0.93	0.98	0.94
10357381	Ysk4	1.10	1.06	1.24	0.90	1.23	0.97	1.35	1.00	4.59E-04	1.00	1.00	1.00	0.73	0.98	0.97
10544150	Jhdm1d	1.35	1.19	1.31	1.00	1.21	1.04	1.36	1.00	5.02E-04	1.00	1.00	1.00	0.78	0.98	0.85
10416251	Egr3	1.22	0.91	1.23	0.91	1.30	1.08	1.39	1.00	5.25E-04	1.00	1.00	1.00	0.39	0.99	1.00
10469425	Arl5b	1.42	1.16	1.30	0.99	1.54	1.15	1.47	1.00	9.28E-04	1.00	1.00	1.00	0.90	0.99	0.29
10378545		1.34	0.75	1.29	0.97	1.27	0.88	1.24	1.00	9.28E-04	1.00	1.00	1.00	1.00	0.98	0.68
10544148	Jhdm1d	1.19	1.04	1.20	0.96	1.20	0.97	1.13	1.00	9.28E-04	1.00	1.00	1.00	0.97	0.99	0.89
10346878	Zdbf2	1.42	1.08	1.29	0.92	1.37	1.03	1.32	1.00	9.97E-04	1.00	1.00	1.00	1.00	0.98	0.54
10449741	Snf1lk	1.28	1.06	1.34	0.99	1.60	1.09	1.64	1.00	1.46E-03	1.00	1.00	1.00	0.61	0.99	0.99
10593492	Zc3h12c	1.22	0.98	1.41	1.08	1.22	0.99	1.26	1.00	1.56E-03	1.00	1.00	1.00	0.88	0.98	0.49
10573198	Dnajb1	1.44	1.09	1.42	1.04	1.48	1.15	1.51	1.00	2.33E-03	1.00	1.00	1.00	1.00	0.99	0.91

10448471	Dnase1l2	1.22	1.06	1.18	1.02	1.16	0.99	1.24	1.00	5.54E-03	1.00	1.00	1.00	0.99	0.98	1.00
10366043	Dusp6	1.27	0.91	1.32	0.96	1.27	1.01	1.36	1.00	5.83E-03	1.00	1.00	1.00	0.97	0.99	0.96
10492428	Tiparp	1.24	1.08	1.26	0.92	1.21	1.03	1.38	1.00	6.54E-03	1.00	1.00	1.00	1.00	0.98	0.99
10510574	Errfi1	1.14	0.96	1.14	0.92	1.26	0.96	1.37	1.00	7.03E-03	1.00	1.00	1.00	0.62	0.98	0.98
10364950	Gadd45b	1.44	1.13	1.62	0.96	1.63	1.31	1.72	1.00	8.26E-03	1.00	1.00	1.00	0.87	0.98	0.90
10502655	Cyr61	1.35	0.77	1.11	0.84	1.56	0.78	1.65	1.00	9.60E-03	1.00	1.00	1.00	0.67	0.98	0.98
10417034	Dnajc3a	1.20	1.07	1.17	1.01	1.17	1.02	1.14	1.00	1.03E-02	1.00	1.00	1.00	0.91	0.98	0.79
10417013	Dnajc3a	1.20	1.07	1.17	1.01	1.17	1.01	1.14	1.00	1.03E-02	1.00	1.00	1.00	0.91	0.98	0.80
10440522	Adamts1	1.01	0.91	1.04	0.89	1.12	1.02	1.29	1.00	1.03E-02	1.00	1.00	1.00	0.04	0.98	0.82
10404595	Ppp1r3g	1.13	0.94	1.13	0.94	1.16	0.98	1.27	1.00	1.03E-02	1.00	1.00	1.00	0.76	0.98	0.94
10412038	Zswim6	1.24	1.10	1.15	0.90	1.29	1.11	1.09	1.00	1.11E-02	1.00	1.00	1.00	0.98	1.00	0.01
10394735	Pdia6	1.19	1.08	1.15	1.02	1.22	1.03	1.15	1.00	1.14E-02	1.00	1.00	1.00	1.00	1.00	0.47
10576971	Irs2	1.12	0.90	1.18	0.94	1.14	0.99	1.21	1.00	1.21E-02	1.00	1.00	1.00	0.83	0.99	0.84
10580282	Junb	1.35	1.04	1.35	1.03	1.36	1.12	1.37	1.00	1.34E-02	1.00	1.00	1.00	1.00	0.98	0.97
10545682	Tet3	1.20	1.00	1.16	0.96	1.33	1.10	1.16	1.00	1.34E-02	1.00	1.00	1.00	0.73	0.98	0.36
10571312	Dusp4	1.09	0.91	1.17	0.99	1.09	0.94	1.28	1.00	1.58E-02	1.00	1.00	1.00	0.97	0.98	0.24
10573626	Gpt2	1.03	1.00	1.09	0.93	1.22	1.03	1.20	1.00	1.63E-02	1.00	1.00	1.00	0.26	0.99	0.97
10516064	Mfsd2	1.18	0.93	1.19	0.95	1.36	1.02	1.36	1.00	1.83E-02	1.00	1.00	1.00	0.66	0.99	1.00
10371400	Cry1	1.24	1.13	1.07	1.00	1.29	1.08	1.16	1.00	2.19E-02	1.00	1.00	1.00	1.00	0.98	0.02
10363350	P4ha1	1.15	1.10	1.28	0.96	1.26	1.04	1.27	1.00	2.29E-02	1.00	1.00	1.00	1.00	1.00	0.98
10543785	AB041803	1.11	0.99	1.40	1.09	1.37	0.98	1.47	1.00	2.71E-02	1.00	1.00	1.00	1.00	0.98	0.49
10543017	Pdk4	1.23	1.07	1.27	0.99	1.32	1.14	1.46	1.00	2.74E-02	1.00	1.00	1.00	0.82	0.99	0.99
10593430	Snf1lk2	1.28	1.10	1.17	0.94	1.33	1.05	1.19	1.00	2.95E-02	1.00	1.00	1.00	1.00	0.98	0.27
10364702	Midn	1.24	1.10	1.11	0.90	1.42	1.09	1.18	1.00	3.06E-02	1.00	1.00	1.00	0.72	0.99	0.07
10530910	Uba6	1.33	1.19	1.22	1.06	1.27	1.00	1.15	1.00	3.16E-02	1.00	1.00	1.00	0.51	0.98	0.37
10572800	Klf2	1.26	1.00	1.16	1.01	1.32	1.03	1.32	1.00	3.31E-02	1.00	1.00	1.00	0.94	0.99	0.98
10520862	Fosl2	1.19	1.05	1.20	1.03	1.32	1.13	1.28	1.00	3.80E-02	1.00	1.00	1.00	0.84	0.98	0.86
10426098	Creld2	1.42	1.17	1.15	0.98	1.25	1.12	1.17	1.00	3.98E-02	1.00	1.00	1.00	0.95	0.98	0.03
10400095	Ifrd1	1.17	1.04	1.22	0.98	1.16	0.98	1.33	1.00	3.98E-02	1.00	1.00	1.00	1.00	0.98	0.91
10344807	Cspp1	1.18	1.11	1.33	1.11	1.40	1.07	1.17	1.00	4.41E-02	1.00	1.00	1.00	1.00	0.98	0.93
10451650	Nfya	1.17	1.07	1.25	1.11	1.18	1.04	1.28	1.00	4.71E-02	1.00	1.00	1.00	0.99	0.99	0.83
10488048	Mkks	1.07	0.94	1.11	1.02	1.10	1.00	1.20	1.00	4.80E-02	1.00	1.00	1.00	0.84	0.99	0.51

Supplemental Materials and Methods:

Animals and treatments

Experiments were performed in adult (3-5 months) C57/DBA F1 hybrid females. Trichostatin A (TSA) (Sigma Aldrich Química S.A.) 2,4 mg/kg in DMSO/Saline solution (1:4) was administered by intraperitoneal injection. We performed a series of preliminary experiments with different doses of TSA (0.6-2.4 mg/kg) as well as with a second HDACi – sodium butyrate (NaBt) (0.15-1.2 g/kg). Although, both drugs produced a pronounced increase of histone acetylation levels in protein extracts, we chose TSA over NaBt because the later severely reduced the activity of the animal in the open arena when used at high doses (data not shown). We chose the higher concentration of TSA (2.4 mg/Kg) because we wanted to have a histone hyperacetylation response as robust as possible without affecting locomotor activity. The generation (55) and neurological characterization (3,20) of $cbp^{+/-}$ mice have been previously described. These mice are maintained in a DBA and C57BL/6J mixed background because they are not viable in a pure C57BL/6J background (3). All mice were housed in 30x15x11 cm clear cages occupied by 4-5 mice and kept on a 12h light/dark cycle; food and water were provided *ad libitum.* The Exposure to novelty consisted of placing an individual animal in a white Plexiglas square box (50×50×30 cm) containing plastic tubing and small toys for 1 h. In the novelty experiment, TSA or vehicle solutions were administrated 15 min before starting the novelty paradigm. Homecage animals were maintained in their cages but otherwise were treated as the novelty groups. Mice were sacrificed immediately after novelty and the hippocampi dissected and treated according to the use given to these animals (see Western blot, ChIP and RT-qPCR sections). Experimental protocols were compliant with European regulations and approved by the Institutional Animal Care and Use Committee.

Western blot analyses

Western blot analyses were carried out as previously described (21,56). The following antibodies were used: acetyl-histone antibodies specific for the panacetylated forms of H2A (K5, K9), H2B (K5, K12, K15, K20), H3 (K9, K14) and H4 (K5, K8, K12, K16) produced in our laboratory (21); α-AcH3K9,14 (06-599), α-H2B (07-371), α-H3 (05-499) from Millipore (Billerica, MA, USA); α -AcH4K12 (ab46983) from Abcam (Cambridge, UK); α-β-actin (F5441) and HRP-conjugated secondary antibodies from Sigma Aldrich Química S.A.

RT-qPCR and microarray analyses

Total hippocampal RNA was purified using TRI reagent (Sigma) and reverse-transcribed using RevertAid First Strand cDNA Synthesis kit (Fermentas, St. Leon-Rot, Germany) according to manufacturers' instructions. Quantitative RT-PCRs (qRT-PCR) assays to validate microarray data were performed in an Applied Biosystems 7300 real-time PCR unit using SYBR GreenER mix (Invitrogen). Each independent sample was assayed in duplicate and normalized using glyceraldehyde 3-phosphate dehydrogenase (GAPDH) levels. All primer sequences are available upon request. For microarray hybridization, total RNA extracted from the hippocampus of 3-4 age, sex and genotype-matched mice were pooled, treated with DNaseI and cleaned up using the RNeasy mini kit (Qiagen, Valencia, CA). Three to five independent pooled samples per genotype, condition and treatment, were hybridized to Mouse Gene 1.0 ST expression arrays (Affymetrix, Santa Clara, CA). The arrays were hybridized, washed and screened for quality according to the manufacturer's protocol. The microarray data were then analysed using GeneSpring GX 11 (Agilent Technologies, Inc., Santa Clara, CA). RMA (Robust Multichip Average) algorithm was used for data normalization. Principal component analysis revealed clustering of

samples according to the batch of replicates; therefore, normalization was conducted using the median of the corresponding control samples values as reference. TCs were then filtered on signal intensity by establishing a lower cutoff at the 20th percentile (20th–100th percentile). Transcripts differentially regulated upon TSA treatment in wild-type mice were identified using unpaired t-test. Novelty-regulated transcripts were identified by three-way ANOVA analysis. In significance analysis, P-values were obtained by asymptotic computation and corrected for multiple testing with Benjamini–Hochberg FDR method. Hierarchical clustering was performed using either GeneSpring software or R 2.15 (http://www.r-project.org/). The following filters were applied: fold change (FC) > 1.2 and adjusted P-value < 0.05. GO enrichment analysis for differentially regulated genes upon TSA was performed using the web-based gene set analysis toolkit (WebGestalt) (57).

ChIP assays and ChIPseq analysis

Chromatin immunoprecipitation (ChIP) was performed as described previously (20). Diluted chromatin was incubated overnight at 4ºC in the presence of specific IgGs against AcH3 (Millipore, 06-599), AcH4K12 (abcam, ab46983), AcH2B (21) or H3K4me3 (Millipore, 07-473) or rabbit-derived pre-immune serum. All these antibodies are residue/s specific and suitable for ChIP assays and ChIP-seq experiments. In particular, anti-AcH4K12 has been validated in previous ChIPseq experiments in the hippocampus (23), and the anti-AcH3 and anti-H3K4me3 are included in the ENCODE project antibody database (http://genome.ucsc.edu/ENCODE/antibodies.html). The AcH3 antibody was produced by immunization with a KLH-conjugated peptide corresponding to amino acids 1-20 of Tetrahymena histone H3 (ARTKQTAR[K*]STGG[K*]APRKQLC) and it is referred to as AcH3K9,14 through the text. The AcH2B antiserum was produced

by our group through repeated subcutaneous injection in rabbits of a KLH-conjugated peptide with residues 1-22 of mouse histone H2B acetylated at the lysine residues in positions 5, 12, 15 and 20. The antiserum has been used in a number of previous studies (20,21,28) and its performance was compared with that of commercial antibodies with the same specificity. In addition, the specificity of the AcH2B antiserum was evaluated by competition assays in the presence of the acetylated or unacetylated form of the peptide used in the production of the antibody (Supplemental Figure S2A). Immunoprecipitation and ChIP experiments show that the rabbit anti-AcH2B antiserum precipitates AcH2B (Figure S2B) and associated DNA (Figure S2C). ChIP-qPCR was performed as described for RT-qPCR using specific primers immediately upstream of the transcription start site (TSS). All primer sequences are available upon request. For ChIPseq, whole hippocampi from 3 mice were pooled in each sample to perform ChIP. High-throughput sequencing of DNA libraries from AcH2B ChIP, vehicle and TSA, was performed using a GAII (Illumina). All the other sample libraries, including 2 additional AcH2B datasets (n=2), AcH3K9,14 (naïve (n=2), vehicle and TSA), AcH4K12 (naïve, vehicle, TSA), H3K4me3, input and IgG were sequenced in HiSeq-2000 apparatus (Illumina). See Table S1 for additional information on library size, preparation and other details. We followed ENCODE recommendations for ChIPseq experiments (58). Reads were aligned to the NCBI-M37/mm9 reference genome using BWA (59) and BAM files were parsed using SAMTOOLS to select uniquely mapped reads (60). Cross-correlation matrix and dendrogram of HiSeq-2000 datasets were generated by using coverage values per kb (counts per million per kb) across the whole genome with Seqmonk (Simon Andrews, Babraham Institute). In addition, two dimension Multi-Dimensional Scaling (MDS) of whole coverage profiles was performed using htSeqTools (61). To extract acetylation-

enriched chromatin regions, paired analysis of datasets from vehicle and TSA-treated mice were performed by using the SICER algorithm (22). To reduce background noise, input and IgG were pooled together to conform the control library used in the peak calling process. SICER parameters for island identification and differential analysis were as follows: redundancy threshold = 100, window size = 200, gap size = 2 (AcH3K9,K14) or 3 (AcH4K12), fragment size = 150, effective genome fraction = 0.77 and FDR = 10^{-8} (AcH3K9,K14 and AcH4K12) or E value = 10 (AcH2B). Two independent biological replicates were merged to generate the AcH2B vehicle dataset used in the differential analysis. Identification of H3K4me3 chromatin-enriched regions was performed with the same settings as AcH3K9,14. Island width analysis was done using the same parameters for all the datasets (w=2, g=3). Overlap and annotation of significantly enriched islands was done with ChipPeakAnno (62). Integrative Genomics Viewer (IGV) (63) were used for data visualization and coverage snapshots at discrete loci. For genome-wide feature analysis, regions of interest were extracted and centered. CBP- and p300-bound sites were obtained from (26,27); graphs show the mean density plotted normalized relative to total number of sequence reads in the corresponding datasets. Density heatmap density plots for the indicated histone modification were determined as counts per million in 25bp bins in the 10 kb region surrounding the TSS. seqMINER (64) was used to generate the heatmaps and k-means clustering data.

Statistical analysis

Quantitative data were analyzed using R 2.15 and SPSS Statistic software V.19 (IBM, Armonk, NY). The data were first subjected to a normality test and an equal variance test. Data that passed these two tests were then analyzed by either ANOVA when comparing several groups or Student's t-test to compare two groups. Cumulative

probability distribution histograms were compared using Kolmogorov-Smirnov test. Sample size is indicated in the description of each experiment and figure legends.

Data access

The files generated in the microarrays and ChIPseq screens are available at the Gene Expression Omnibus (GEO) database with the accession number GSE44868.

References

55. Tanaka, Y., Naruse, I., Maekawa, T., Masuya, H., Shiroishi, T. and Ishii, S. (1997) Abnormal skeletal patterning in embryos lacking a single Cbp allele: a partial similarity with Rubinstein-Taybi syndrome. *Proc Natl Acad Sci U S A*, **94**, 10215-10220.
56. Lopez de Armentia, M., Jancic, D., Olivares, R., Alarcon, J.M., Kandel, E.R. and Barco, A. (2007) cAMP response element-binding protein-mediated gene expression increases the intrinsic excitability of CA1 pyramidal neurons. *J Neurosci*, **27**, 13909-13918.
57. Zhang, B., Kirov, S. and Snoddy, J. (2005) WebGestalt: an integrated system for exploring gene sets in various biological contexts. *Nucleic Acids Res*, **33**, W741-748.
58. Landt, S.G., Marinov, G.K., Kundaje, A., Kheradpour, P., Pauli, F., Batzoglou, S., Bernstein, B.E., Bickel, P., Brown, J.B., Cayting, P. *et al.* (2012) ChIP-seq guidelines and practices of the ENCODE and modENCODE consortia. *Genome Res*, **22**, 1813-1831.
59. Li, H. and Durbin, R. (2010) Fast and accurate long-read alignment with Burrows-Wheeler transform. *Bioinformatics*, **26**, 589-595.
60. Li, H., Handsaker, B., Wysoker, A., Fennell, T., Ruan, J., Homer, N., Marth, G., Abecasis, G. and Durbin, R. (2009) The Sequence Alignment/Map format and SAMtools. *Bioinformatics*, **25**, 2078-2079.
61. Planet, E., Attolini, C.S., Reina, O., Flores, O. and Rossell, D. (2012) htSeqTools: high-throughput sequencing quality control, processing and visualization in R. *Bioinformatics*, **28**, 589-590.
62. Zhu, L.J., Gazin, C., Lawson, N.D., Pages, H., Lin, S.M., Lapointe, D.S. and Green, M.R. (2010) ChIPpeakAnno: a Bioconductor package to annotate ChIP-seq and ChIP-chip data. *BMC Bioinformatics*, **11**, 237.
63. Robinson, J.T., Thorvaldsdottir, H., Winckler, W., Guttman, M., Lander, E.S., Getz, G. and Mesirov, J.P. (2011) Integrative genomics viewer. *Nature biotechnology*, **29**, 24-26.
64. Ye, T., Krebs, A.R., Choukrallah, M.A., Keime, C., Plewniak, F., Davidson, I. and Tora, L. (2011) seqMINER: an integrated ChIP-seq data interpretation platform. *Nucleic Acids Res*, **39**, e35.